Available online at www.sciencedirect.com
ScienceDirect
Trans. Nonferrous Met. Soc. China 19(2009) 1342−1347
Transactions of Nonferrous Metals Society of China
www.tnmsc.cn

Recovery of alumina and ferric oxide from Bayer red mud rich in iron by reduction sintering

LI Xiao-bin(李小斌), XIAO Wei(肖 伟), LIU Wei(刘 伟), LIU Gui-hua(刘桂华), PENG Zhi-hong(彭志宏), ZHOU Qiu-sheng(周秋生), QI Tian-gui(齐天贵)

School of Metallurgical Science and Engineering, Central South University, Changsha 410083, China

Received 11 September 2008; accepted 17 December 2008

Abstract: A great amount of red mud generated from alumina production by Bayer process not only threatens the environment but also causes waste of secondary resources. High-iron-content red mud from Bayer process was employed to recover alumina and ferric oxide by the process of reduction-sintering, leaching and then magnetic beneficiation. Results of thermodynamic analyses show that ferric oxide should be reduced to Fe if reduction of ferric oxide and formation of sodium aluminate and calcium silicate happen simultaneously. Experimental results indicate that alumina recovery of Bayer red mud can reach 89.71%, and Fe recovery rate and the grade of magnetite concentrate are 60.67% and 61.78%, respectively, under the optimized sintering conditions.
Key words: high iron content; red mud; recovery; reduction; sintering; magnetic beneficiation

1 Introduction

Red mud, which contains considerable amount of alumina, caustic soda, ferric oxide, titania and other minor valuable constituents, is the major waste material of the alkaline extraction of alumina from bauxite by Bayer process[1]. At present, about 6×10^7 t of red mud is discharged to the environment every year all over the world[2]. A mass of red mud not only occupies precious land, but also threatens the environment because of basifying land and polluting underground water. So, treating and disposal of red mud has attracted much attention[3]. Up to now, many researchers have carried out a lot of studies on the effective or comprehensive utilization of red mud, and a variety of ways has been proposed to deal with red mud of different chemical compositions as well as phase components [4−7], such as high pressure hydro-chemistry method[8], reduction roasting[9−10], direct magnetic separation[11]. As far as high pressure hydro-chemistry method is concerned, red mud is leached at high temperature (＞260 ℃) and high alkalinity (molar ratio of Na_2O to Al_2O_3＞10) to recover caustic soda and alumina, where ferric oxide in red mud cannot be recovered. And it has not yet been applied in industry for more than half a century of research because of its technical and economic reasons, such as facility corrosion at high temperature and low alumina concentration in the resultant solution after leaching. The main purpose of reduction roasting and direct magnetic separation is to recover ferric oxide from red mud without consideration of recovery of caustic soda and alumina. Furthermore, as for the direct magnetic separation method, the grade of magnetite concentrate obtained from red mud and iron recovery ratio are relatively low, approximately 55% and 35%, respectively.

Recovery of caustic soda, alumina and ferric oxide is a fundamental way to comprehensively utilize red mud. Sintering method is an effective way to deal with aluminum-containing raw materials with low mass ratio of alumina to silica, and it facilitates iron recovery in the sintering process[12]. However, there are still many problems to simultaneously recover caustic soda, alumina and ferric iron from red mud by sintering. Firstly, red mud rich in iron has a quite low mass ratio of alumina to silica (A/S＜1.5) as well as high iron content ($w(Fe_2O_3)$＞35%), which is readily to form colliquable eutectic so as to decrease melting point of furnace charge and narrow sintering temperature range. Secondly, ferric oxide (mainly hematite), silica and alumina in red mud should be converted into magnetite, calcium silicates and

Foundation item: Project(2005CB623702) supported by the National Basic Research Program of China
Corresponding author: LIU Wei; Tel: +86-731-88830453; E-mail: qtg_csu@163.com
DOI: 10.1016/S1003-6326(08)60447-1

sodium aluminate, respectively, at the same time in order to economically recover ferric oxide and alumina during sintering process. But there are few work reported in this field, so it is necessary to study the behavior of high-iron-content red mud in the sintering process in order to effectively utilize it.

2 Experimental

2.1 Materials

The main chemical compositions of the high-iron-content Bayer red mud used in the experiments are listed in Table 1.

Table 1 Main chemical compositions of red mud (mass fraction, %)

Fe_2O_3	Al_2O_3	SiO_2	CaO	TiO_2	Na_2O
32.52	18.42	8.34	16.74	6.75	3.59

The main phases of red mud are hydrate garnet ($Ca_3(Al_{0.13}Fe_{0.87})_2(SiO_4)_{1.15}(OH)_{5.4}$), diasporite (AlOOH), gibbsite ($Al(OH)_3$), hematite (α-Fe_2O_3) and goethite (α-FeOOH).

2.2 Experimental method

Quantitative red mud, carbon, soda ash, lime were weighed according to the prescription of furnace charge and then filled in a 500 mL plastic bottle containing ten *d* 15 mm steel balls. Then the bottle was placed on a roller-crushing mill to mix the raw materials for 2 h. Some of the mixed furnace charge was taken out and placed into a crucible, then preheated at 800 ℃ for 20 min in the muffle furnace. After being preheated, the furnace charge was sintered under experimental conditions and transformed to sinter. Then, the sinter was kept in another muffle furnace at 600 ℃ for 20 min then was cooled to the room temperature. In the end, the sinter was weighed, ground and then held in a sealed glass bottle for leaching.

3 Thermodynamic analyses

When the carbon is introduced to the process, Al_2O_3, SiO_2, CaO or Na_2O in red mud does not react with it. The reactive rules of iron-containing compounds with carbon were thermodynamically analyzed. Table 2 lists various reactions of iron-containing compounds, and their relationships between ΔG^{Θ} calculated according to thermodynamic data[13−14] and temperature in the reduction sintering process. According to the relationship between ΔG^{Θ} and reaction equilibrium constant, and the relationship between reaction equilibrium constant and gas equilibrium component of reactions (1)−(5), the equilibrium phase diagram of ferric oxides reduced by carbon can be drawn as Fig.1 when the pressure is 1.013×10^5 Pa, where serial numbers beside the curves represent corresponding reactions as shown in Table 2.

Reaction (1) is the carbon gasification reaction and its degree of freedom is 2, so its gas equilibrium components in the reaction depends on the reaction temperature and the total pressure. Fig.1 shows the isotonic curve of gas equilibrium components of reaction (1). As shown in Fig.1, when there is excessive carbon in sintering process, the higher the temperature, the higher

Table 2 Possible chemical reactions and their relationship between ΔG^{Θ} and temperature during reduction sintering of high-iron-content red mud

Reaction number	Chemical reaction	$\Delta G^{\Theta}/(\mathrm{kJ\cdot mol^{-1}})$
(1)	$CO_2+C=2CO$	$\Delta G^{\Theta}_{(1)}=170.71-0.175T$
(2)	$3Fe_2O_3+CO=2Fe_3O_4+CO_2$	$\Delta G^{\Theta}_{(2)}=-52.131-0.041\ 0T$
(3)	$Fe_3O_4+CO=3FeO+CO_2$	$\Delta G^{\Theta}_{(3)}=35.38-0.040\ 2T$
(4)	$FeO+CO=Fe+CO_2$	$\Delta G^{\Theta}_{(4)}=-13.18+0.017\ 2T$
(5)	$(1/4)Fe_3O_4+CO=(3/4)Fe+CO_2$	$\Delta G^{\Theta}_{(5)}=-3.26+0.004\ 21T$
(6)	$Fe_2O_3+Na_2CO_3=Na_2O\cdot Fe_2O_3+CO_2$	$\Delta G^{\Theta}_{(6)}=143.50-0.158T$
(7)	$Fe_2O_3+CaO=CaO\cdot Fe_2O_3$	$\Delta G^{\Theta}_{(7)}=-21.55-0.014\ 9T$
(8)	$2CaO+Fe_2O_3=2CaO\cdot Fe_2O_3$	$\Delta G^{\Theta}_{(8)}=-42.08-0.021\ 1T$
(9)	$Fe_2O_3+3C=2Fe+3CO$	$\Delta G^{\Theta}_{(9)}=478.54-0.516T$
(10)	$Na_2O\cdot Fe_2O_3+2C=Na_2CO_3+2Fe+CO$	$\Delta G^{\Theta}_{(10)}=161.64-0.209T$
(11)	$CaO\cdot Fe_2O_3+3C=CaO+2Fe+3CO$	$\Delta G^{\Theta}_{(11)}=500.10-0.501T$
(12)	$2CaO\cdot Fe_2O_3+3C=2CaO+2Fe+3CO$	$\Delta G^{\Theta}_{(12)}=520.60-0.494T$

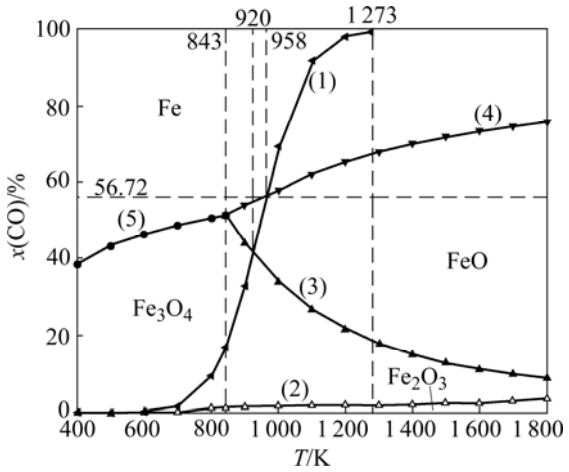

Fig.1 Phase equilibrium diagram of iron oxides during carbon reduction process

the CO content in the equilibrium gas phase. Reactions (2)−(5) are reduction reactions of ferric oxides. The pressure has no effect on the equilibrium of these reactions because the degree of freedom is 1, and their gas equilibrium components are controlled by reaction temperature. When the temperature is lower than 1 273 K, CO and CO_2 coexist in the equilibrium components of the carbon gasification reaction. When the temperature is higher than 1 273 K, the concentration of CO_2 is very low and the concentration of CO is far higher than that of CO_2. Equilibrium curves of reactions (2)−(5) divide the ferric oxide equilibrium phase graph into four regions of Fe_2O_3, Fe_3O_4, FeO and Fe, respectively. As shown in the equilibrium phase diagram, the temperature should be controlled below 920 K in order to convert ferric compounds to the form of magnetite. However, it is difficult to form calcium silicates under such a low temperature, because the regular sintering temperature for bauxite is higher than 1 270 K[9].

The formation of sodium ferrite or calcium ferrite shown in reactions (6)−(8) is common in the sintering process of bauxite. Once these reactions happen, ferric minerals in slag after sinter leaching have no magnetism, which is not favorable to iron recovery. Therefore, the sintering conditions should be controlled to ensure Fe_2O_3 to be reduced as reaction (9) as much as possible. Thermodynamic calculation results of reactions (6)−(9) in the standard state are shown in Fig.2. The formation of calcium ferrite has precedence over the formation of sodium ferrite, and when the temperature is higher than 1 053 K, carbon reduction reaction from Fe_2O_3 to Fe takes precedence over the formation of ferrite.

In Fig.2, it should be noted that $2CaO{\cdot}Fe_2O_3$, $CaO{\cdot}Fe_2O_3$ and $Na_2O{\cdot}Fe_2O_3$ may be formed preferentially during sintering process when the temperature is below 1 053 K. Therefore, it is necessary to study reactions (10)−(12) that $2CaO{\cdot}Fe_2O_3$, $CaO{\cdot}Fe_2O_3$ and $Na_2O{\cdot}Fe_2O_3$ are reduced by carbon, and the corresponding thermodynamic calculation results are shown in Fig.3. As shown in Fig.3, when the sintering temperature is higher than 1 053 K, the values of ΔG of the ferrite reduction reactions in the furnace burden are negative, indicating that ferric compounds in red mud can completely be transformed into element iron under normal sintering temperature.

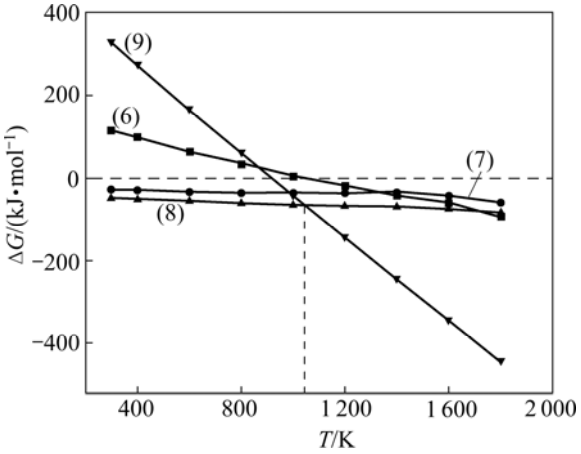

Fig.2 Relationships between ΔG and temperature during formation of ferrite

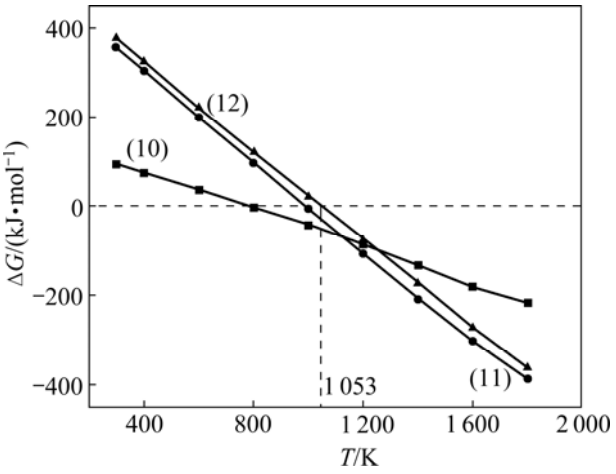

Fig.3 Relationships between ΔG and temperature of carbon reduction reaction of ferrite

From the above thermodynamic calculation and analyses, the conclusion may be made that the reduction reactions of ferric minerals can be realized by controlling the atmosphere in the sintering process of high-iron-content furnace burden at the temperature for the formation of sodium aluminum and calcium silicates.

4 Results and discussion

4.1 Effects of sintering temperature and time on alumina recovery of sinter

Sintering temperature and duration time have an important influence on the quality of sinter during sintering process. When the amount of carbon added (the mass ratio of carbon to total raw materials) is 20%, Fig.4 shows the effect of sintering temperature and sintering time on alumina recovery rate of sinter. It is shown that alumina recovery rate of sinter increases with the increase of sintering temperature or prolongation of sintering time. When there are Na_2CO_3, Al_2O_3 and Fe_2O_3 in the furnace charge, Fe_2O_3 of $Na_2O{\cdot}Fe_2O_3$ could be replaced thermodynamically by Al_2O_3 to generate $Na_2O{\cdot}Al_2O_3$ during sintering process[15]. This replacement reaction helps to increase alumina recovery rate of sinter, and the replacement reaction degree increases with the increase of temperature and the prolongation of sintering time. However, when sintering temperature is higher than 1 323 K, alumina recovery rate decreases rapidly because the residual $Na_2O{\cdot}Fe_2O_3$ reacts with calcium silicate and calcium ferrite in the furnace charge to form sosoloid, which decreases the melting point to form lots of liquid in advance and further hinder the sintering reaction[9]. Too long sintering time (about 120 min) also has a negative effect on alumina recovery rate. The possible reason for this is that the reduced iron is oxidized again to form Fe_2O_3 and then Fe_2O_3 reacts with $2CaO{\cdot}SiO_2$ to form $CaO{\cdot}SiO_2$, and finally $CaO{\cdot}SiO_2$ reacts with $Na_2O{\cdot}Al_2O_3$ to form a ternary compound when the reductant exhausts[15].

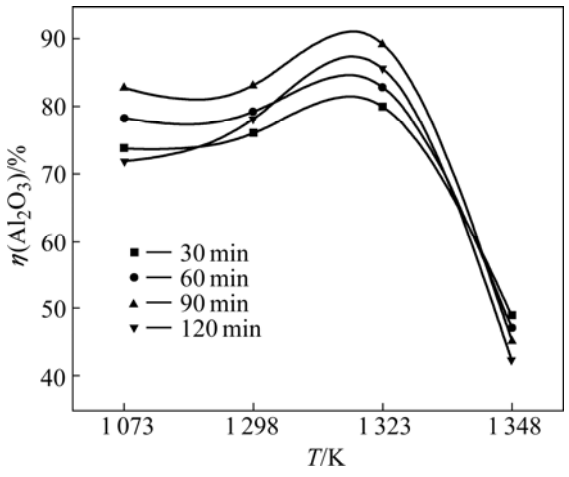

Fig.4 Effect of sintering temperature and time on alumina recovery rate of sinter

4.2 Influence of amount of carbon added in furnace charge on alumina recovery rate of sinter

Fig.5 illustrates the influence of amount of carbon added on alumina recovery rate of the sinter sintered at 1 323 K. It is indicated that both increasing amount of carbon added and prolonging sintering duration time can promote alumina recovery rate of sinter. With the increase of amount of carbon added in the furnace charge, iron compounds can be reduced more completely, which can prevent the formation of $Na_2O{\cdot}Fe_2O_3$ to a great extent. Furthermore, CO_2 generated from the reaction of alumina with sodium carbonate reacts with carbon to form CO, which favors the reaction of alumina with sodium carbonate to form sodium aluminate so as to increase the alumina recovery rate of the sinter.

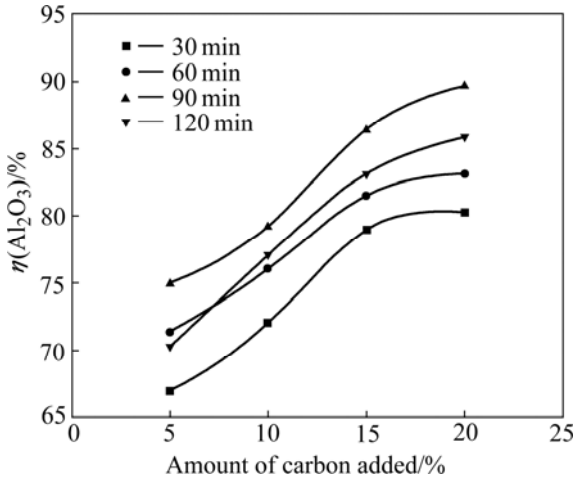

Fig.5 Effect of amount of carbon added on alumina recovery rate of sinter

4.3 Conversion of iron-containing compounds in reduction sintering process

Thermodynamic calculation results show that the ferric compounds in the furnace charge could be reduced into iron so as to isolate iron from the other materials by magnetic beneficiation only when the reductant in the sinter is sufficient during sintering. The reduction of ferric oxide undergoes several steps at high temperature and the amount of the reductant has an important impact on the iron phase in the sinter. X-ray diffraction patterns (in Fig.6) of sinters with 5% and 20% carbon added on the mass of the furnace charge, respectively, show that phases of iron-containing compounds in the sinter are $CaFe_5O_7$, $CaO{\cdot}Fe_2O_3$ and $2CaO{\cdot}Fe_2O_3$ (as shown in Fig.6(a)) with no element iron when the amount of carbon added is 5% on the mass of the total furnace charge. As calcium ferrite has no property of magnetism, it cannot separate iron-containing materials from other materials by magnetic beneficiation, which results in the decrease of recovery rate of Fe. When the amount of carbon added is increased up to 20% on the mass of furnace feed, the phase of calcium ferrites in sinter completely disappears and ferric oxides are reduced into iron(as shown in Fig.6(b)). It is shown that ferric oxide in red mud can be converted into iron when there is enough carbon, and alumina and silica can be converted into $Na_2O{\cdot}Al_2O_3$ and $2CaO{\cdot}SiO_2$, respectively. Thus the recovery of alumina and Fe from high-iron-content red mud can be smoothly realized.

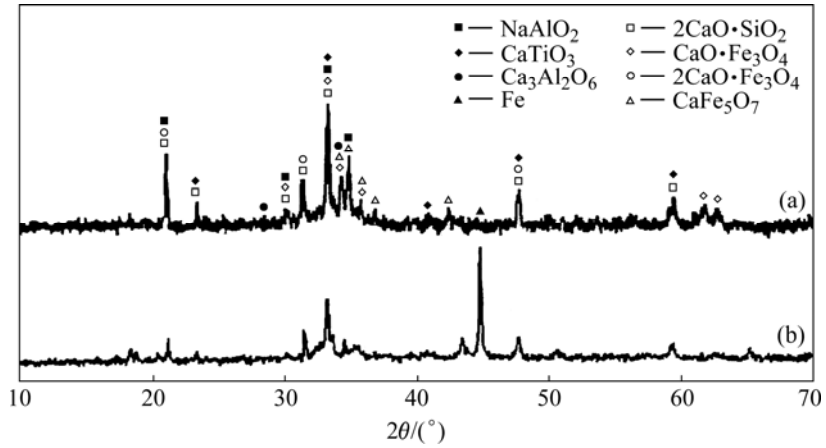

Fig.6 XRD patterns of sinter with different amount of carbon added: (a) 5%; (b) 20%

Fig.7 shows the experimental result of magnetic beneficiation of the leached residue of the sinter prepared at 1 323 K for 90 min with 20% carbon added on the mass of the charge. It can be seen that increasing magnetic field intensity can decrease the grade (TFe) of magnetite concentrate and increase the Fe recovery rate. The reason is that magnetic beneficiation process of magnetic particles is enhanced so that some weak magnetic substance and Fe-entrapped substance are also chosen as magnetite concentrate with increasing magnetic field intensity. With magnetic field of 48 kA/m, magnetite concentrate grade (TFe) reaches 61.78% and the recovery of iron is 60.67%, both of which are much higher than those with direct magnetic separation from red mud operated in some alumina refineries at present. Therefore, the leached residue of the sinter generated from reduction sintering has a satisfactory Fe selectivity. X-ray diffraction patterns, as shown in Fig.8, of the leached residue, tailings and magnetite concentrate also show that the separation of alumina and iron from high-iron-content red mud can be accomplished by the process of reduction sintering, leaching and then magnetic beneficiation.

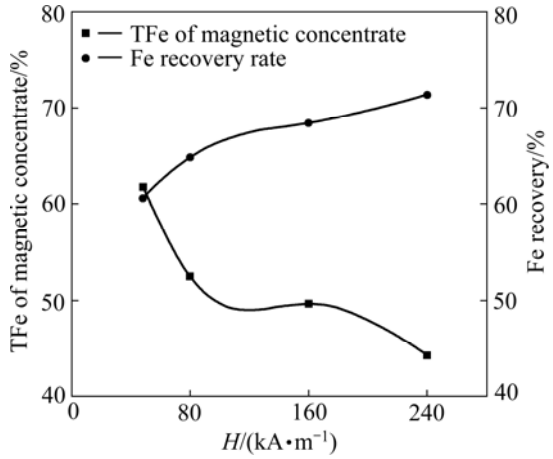

Fig.7 Influence of magnetic field intensity on grade of magnetite concentrate and Fe recovery

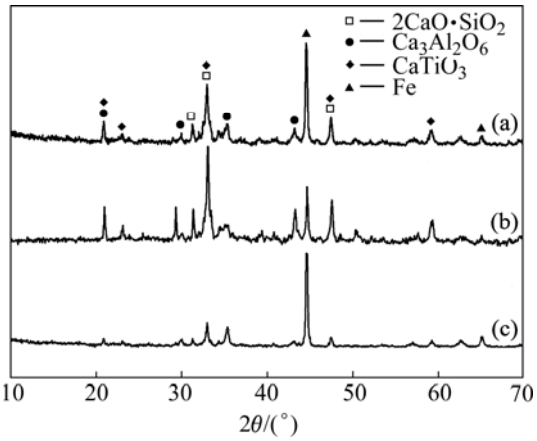

Fig.8 XRD patterns of leached residue, tailings and magnetite concentrate: (a) Leached residue; (b) Tailing; (c) Magnetite concentrate

5 Conclusions

1) Thermodynamic analyses show that ferric oxide can be reduced into magnetite by controlling the atmosphere during the sintering process of high-iron-content red mud with carbon as the reductant. Therefore, reduction sintering of high-iron-content red mud to recover alumina and iron is theoretically possible.

2) Sintering temperature and amount of carbon added have a great influence on alumina recovery. High sintering temperature (>1 323 K) greatly reduces alumina recovery, whereas increasing the amount of carbon added promotes alumina recovery.

3) Ferric oxide in red mud from Bayer process can be completely reduced by adjusting the amount of carbon added into the furnace charge during reduction sintering process. With the increase of amount of carbon added, ferric oxide can be completely reduced and finally

changed into element iron.

4) By employing the process of reduction sintering, leaching and magnetic separation, alumina recovery can reach 89.71%, and Fe recovery and the grade of magnetite concentrate are 60.67% and 61.78%, respectively, under the optimized conditions.

References

[1] PARAMGURU R K, RATH P C, MISRA V N. Trends in red mud utilization — A review [J]. Mineral Processing and Extractive Metallurgy Review, 2005, 26(1): 1−29.

[2] AHMET A. Potential uses of red mud in metallurgical applications [C]// Proceedings of the 3rd International Powder Metallurgy Conference. Ankara. Turkey: Turkish Power Metallurgy Association, TPMA, 2002: 264−272.

[3] SMITH N J, BUCHANAN V E, OLIVER G. The potential application of red mud in the production of castings [J]. Mater Sci Eng A, 2006, 420(2): 250−253.

[4] YALCIN N, SEVINE V. Utilization of bauxite waste in ceramic glazes [J]. Ceramics International, 2000, 26(5): 485−493.

[5] KASLIWAL P, SAI P S T. Enrichment of titanium dioxide in red mud: A kinetic study [J]. Hydrometallurgy, 1999, 53(1): 73−87.

[6] LIU Gui-hua, ZHANG Ya-li, PENG Zhi-hong, ZHOU Qiu-sheng, LIU Xiang-min, LI Xiao-bin. Alumina recovery from sodium hydrate alumino-silicate [J]. The Chinese Journal of Nonferrous Metals, 2004, 14(3): 499−503. (in Chinese)

[7] ZHOU Qiu-sheng, FAN Kuang-sheng, LI Xiao-bin, PENG Zhi-hong, LIU Gui-hua. Alumina recovery from red mud with high iron by sintering process [J]. Journal of Central South University: Science and Technology, 2008, 39(1): 92−97. (in Chinese)

[8] YANG Zhong-yu. Alumina production technology [M]. Beijing: Metallurgical Industry Press, 1981. (in Chinese)

[9] LIU Wan-chao, YANG Jia-kuan, XIAO Bo. Recovering iron and preparing building material with residues from Bayer red mud [J]. The Chinese Journal of Nonferrous Metals, 2008, 18(1): 187−192. (in Chinese)

[10] KUMAR S, KUMAR R, BANDOPADHYAY A. Innovative methodologies for the utilization of wastes from metallurgical and allied industries [J]. Resources, Conservation and Recycling, 2006, 48(4): 301−314.

[11] GUAN Jian-hong. Study on using the high-gradient magnetic separator to recover iron in the red mud [J]. Jiangxi Nonferrous Metals, 2000, 14(4): 15−18. (in Chinese)

[12] MISHRA B, STALEY A, KIRKPATRICK D. Recovery of value-added products from red mud [J]. Minerals and Metallurgical Processing, 2002, 19(2): 87−94.

[13] HUANG Xi-you. Principle of metallurgy [M]. Beijing: Metallurgical Industry Press, 2007: 285. (in Chinese)

[14] BARIN I, KNACKE O. Thermochemical properties of inorganic substances Ⅱ [M]. Heidelberg: Springer-Verlag, 1991: 57−998.

[15] ZHOU Qiu-sheng, QI Tian-gui, PENG Zhi-hong, LIU Gui-hua, LI Xiao-bin. Thermodynamics of reaction behavior of ferric oxide during sinter-preparing process [J]. The Chinese Journal of Nonferrous Metals, 2007, 17(6): 973−977. (in Chinese).

(Edited by YANG Hua)